

Enhancement of Natural Flax Fibers' Mechanical Properties via Supercritical Fluid Treatment

Honors Capstone Report

Jonah Berman, Amy Langhorst, Prof. Alan Taub

Introduction

In recent decades, climate change and greenhouse gas emissions have been the subject of numerous scientific studies. Carbon dioxide, a major heat-trapping gas, has been emitted into the Earth's atmosphere by anthropogenic activities such as fossil-fuel burning since the industrial revolution. The Paris Climate Agreement in 2015 set a consensus target of limiting the global temperature rise to 1.5°C from pre-industrial levels in order to avoid the most severe consequences of climate change [1]. These include extreme weather events such as hurricanes, floods, droughts, wildfires, and ensuing disruptions to agriculture. Furthermore, the climate crisis is disproportionately caused by wealthier developed nations and corporations whose industrial activity has both enriched them and polluted the planet. However, it is not typically the culprits who suffer the most from climate change. Instead, lower income and less developed nations and communities are the ones who are disproportionately affected by climate change through devastating storms, famines, and infrastructure damage [2].

The United States emits more greenhouse gases than almost any other country, with only China above them in that regard [3]. The transportation sector accounts for over 25% of all emissions, with light-duty vehicles, such as cars, trucks, and vans, consuming more energy than all other types of vehicles combined [4]. With the average consumer becoming increasingly concerned with climate change and activists putting pressure on legislators to give the subject more attention, automotive companies are focusing significant resources towards reducing their carbon footprint. One important strategy for automakers to reduce carbon emissions from their vehicles is to reduce their weight, thereby improving fuel economy. In addition, battery electric vehicles (BEV) are even more responsive to weight reduction than internal combustion vehicles (ICV), due to the lower energy density of their batteries compared to liquid fuels. In fact, a 10% reduction in vehicle weight results in just a 6% improvement in fuel economy for ICVs, but the same weight reduction in a BEV translates to a 14% range improvement [5]. The Inflation Reduction Act of 2022 has provided Clean Vehicle Credits to accelerate the shift from ICVs to BEVs, with the hope of achieving 50% EV market share by 2030 [6]. In my own experience working as an intern with Shape Corporation, a tier 1 automotive supplier, the shift to BEVs is an all-consuming issue that has grown exponentially in recent years. Thus, the auto industry is already keen on shaving weight to improve fuel economy and moving towards a landscape that is even more geared towards lightweighting.

Lightweight materials have driven advances in the automotive industry, with low density metals such as aluminum replacing some heavier steel parts. Breakthroughs in composite material technology have led to more car parts being made from lightweight composites. In fact, Shape Corp manufactured the industry's first curved, pultruded carbon-fiber bumper for GM's 2020 Corvette Stingray [7]. Automakers have recently invested in creating parts using bio-based polymeric composite materials reinforced with natural fibers. This is because natural fibers are

lightweight, low cost, and renewable; not only can their low density help improve vehicle fuel economy, but replacing synthetic fibers with natural ones allows automakers to produce cars with carbon-negative parts. As such, Ford has built parts using wheat straw and cellulose, BMW has made composites using bamboo, and Porsche has manufactured composite parts reinforced with flax fibers [8]. So why aren't more car parts being made with natural fiber-reinforced composite materials?

To compare among materials with different densities, we often use "specific" properties, normalized to account for density. While flax fibers have reported values for specific properties that are competitive with glass fibers, the high variability inherent to natural fibers is a major disadvantage (Table 1). This variability can come from weather conditions, plant species, time of harvest, or fiber extraction technique, and poses a significant challenge to engineers trying to design a structural part whose performance must exceed a certain metric. Therefore, synthetic fibers made in precise and repeatable laboratory conditions have been the preferred material reinforcement in composites. Natural fibers are simply too unpredictable in their performance, and the lower bounds of their properties must be considered, especially when designing a car part intended to save lives in a crash. That's why the aforementioned examples of natural fiber reinforced composites in automotive parts were used in non-structural applications, such as indoor aesthetic panels.

Table 1: Properties of natural fibers in comparison to glass fiber, as reported in literature. [9]

Properties	E-glass	Flax	Hemp	Cotton	Bamboo
Density (ρ) (g/cm ³)	2.55	1.3-1.5	1.48	1.5	1
Tensile strength (MPa)	2400	800-1500	550-1110	287-800	391-860
Specific strength (MPa/ ρ)	940	138-965	100-750	191-533	100-860
Elongation (%)	3	1.2-1.6	2-3	3-10	1.7-1.9
Modulus (GPa)	73	20-80	30-60	5.5- 13	18-46
Specific Modulus (GPa/ ρ)	29	18-53	39-47	3.7-8.4	18-46

This study seeks to develop a novel treatment technique to improve the mechanical properties of flax fibers, such that they could be used to replace glass fibers in structural polymer composite applications. Notably, we will be focusing on tensile strength and modulus, which is a measure of stiffness. There were several questions that arose at the beginning of this project;

can a treatment make natural fibers competitive with glass fibers' performance? Can it reduce the variability in their properties to make them more reliable reinforcements in composites? Will the treatment be too expensive for consideration in large-scale, commercial applications such as vehicle manufacturing? After all, one of the advantages of natural fibers over synthetic ones is their lower cost.

Flax fibers used for reinforcement in composites are commonly referred to as technical fibers. The technical fiber consists of individual plant cells (elementary fibers), bound together with a pectin-rich interface called the middle lamella. Flax fibers contain a crystalline (stiffer) cellulosic inner portion surrounded by an amorphous (compliant) middle lamella layer that acts as the glue between cells (Figure 1). There is also a large internal pore called lumen that, along with other porosity in the fibers, act as stress concentrations upon loading and lead to fiber failure. The inherent weakness of the middle lamella also causes cracks to propagate between cells, reducing the fiber's performance [10]. Supercritical fluid has been explored as a treatment technique to improve fiber properties for its ability to modify the fiber surface, extract non-cellulosic components and swell amorphous regions [11]. However, previous studies had found that supercritical fluid treatment had resulted in fiber damage and reduced mechanical performance due to high temperatures, flow rates and moisture. Thus, we decided to investigate a treatment with lower flow rates, temperature, and moisture content to try avoiding the damage reported in other studies.

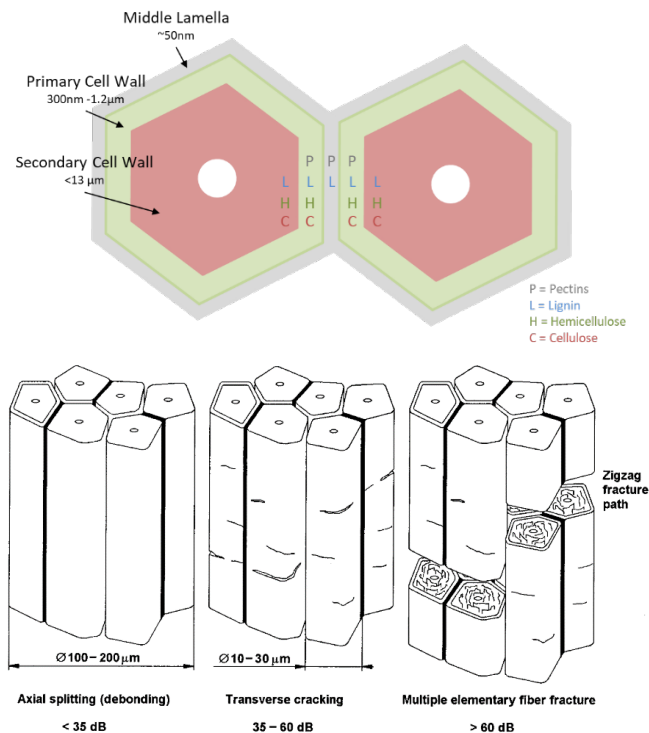


Figure 1: Schematic of fiber morphology; common fracture mechanics at fiber interfaces

Methods

Flax Fibers

Long line technical Agatha flax fibers were grown in Oregon, USA (Fibrevolution, LLC, Portland, OR, USA). The flax stems were dew retted, hand scutched, and hand hackled to yield fibers used throughout this study.

Supercritical Fluid Treatments

A supercritical fluid pressure vessel consisting of the design shown in Figure 2 was used to treat flax fiber samples. Within the pressure vessel, a magnetic stir rod was placed beneath a cage of fiberglass mesh (~1 cm openings) to allow for continuous stirring of the fluid throughout the treatment duration (Figure 2). Prior to treatment, fibers were cut to 6 cm length (unless otherwise stated) and dried for at least 2 hours in a convection oven at 60°C. Samples were placed on top of the fiberglass mesh to prevent damage from the stir-rod during infusion. Samples were treated per the conditions outlined in Table 2. Pressurization occurred at a rate of ~7 kPa/s (1 psi/s).

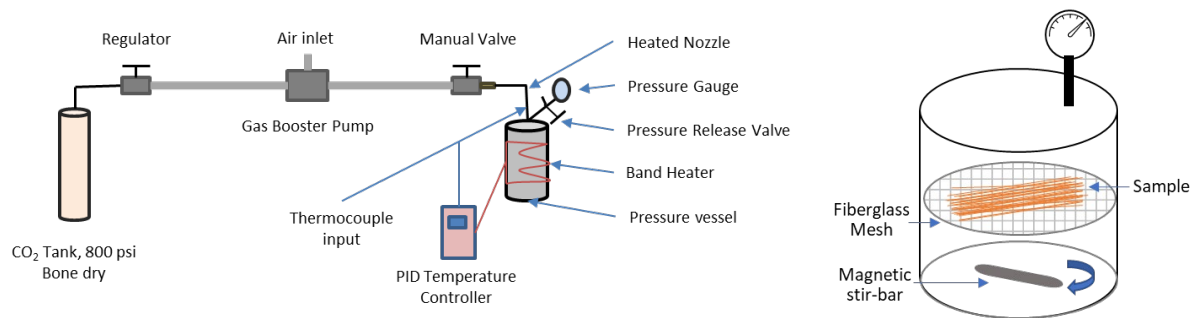


Figure 2: Design of pressure vessel used for supercritical treatment; inside of pressure vessel, with magnetic stir-bar and fiberglass mesh to protect sample.

Table 2: Experimental design for treatment of flax fibers with supercritical fluids

Sample Name	Fluid Type	Pressure [MPa]	Time Duration [hr]	Temperature [°C]	Depressurization rate [kPa/s]
Untreated	-	Untreated	-	-	-
scCO ₂	CO ₂	27.6 (4000 psi)	24	60	35 (5 psi/s)

Single Fiber Tensile Testing

Fibers were mounted in paper frames as shown in Figure 3 per ASTM C1557-20 [12]. To glue the fibers to the frame and prevent slipping during testing, 1-2 drops of 3M General Use No Run Super Glue were applied to the top and bottom edges of the window. A second frame was

applied on top of the first to secure the fiber. At least 20 fibers were mounted and tested per sample. After mounting, all fibers were conditioned in a desiccator box held at 25% relative humidity (RH) for at least 24 hours prior to testing. All fibers were tested at a gauge length of 10 mm.

The cross-sectional area of each fiber mounted for single fiber tensile testing was obtained via imaging of fiber diameters using an Olympus inverted GX51 microscope at 5x magnification followed by image analysis using the software ImageJ Fiji. The diameter of each fiber was measured along two axes as shown in Figure 3. At least 8 measurements were taken along the length of the fiber on each axis and averaged. The fiber cross-sectional area was approximated as the area of an ellipse via Equation 1, as shown in prior studies [13]. Single fiber tensile tests of technical flax fibers were performed according to ASTM C1557-20 on a TA XT Plus Texture Analyzer using a 5kg load cell and an extension rate of 0.01 mm/s [12].

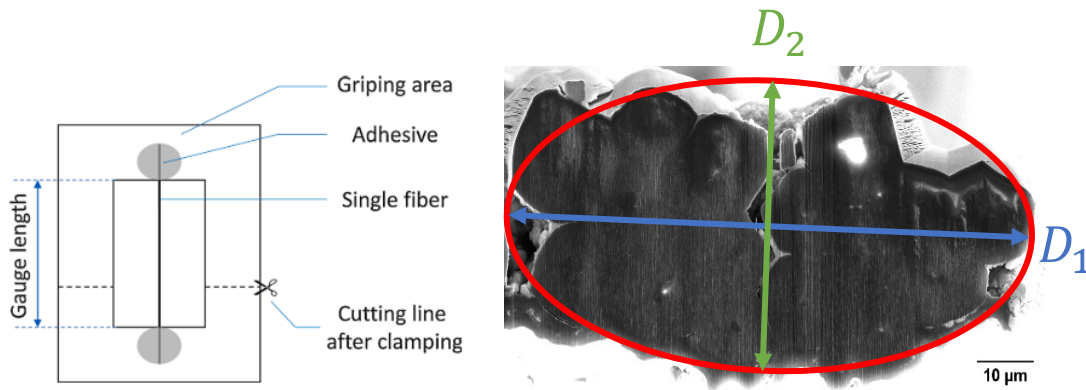


Figure 3: Schematic of paper mount used for single fiber tensile testing of flax fibers; Schematic of diameter measurement locations on fiber. The fibers' cross-sections were approximated as ellipses.

$$A = \pi \cdot \frac{d_1}{2} \cdot \frac{d_2}{2} \quad (1)$$

Porosity & Specific Surface Area

Fiber microporosity and specific surface area were determined via nitrogen physisorption on a Micromeritics ASAP 2020. Fibers were manually cut into a fine powder (< 1mm fiber length) using sharp scissors; at least 0.1 g of fiber were analyzed. Fibers were degassed at 60°C for 2 hours prior to measurement.

Fiber Morphology: Fiber Fixation, Microtoming, & Image Analysis

Fibers underwent fixation and mounting in polymerase chain reaction tubes (PCR) to enable ultramicrotoming and optical microscopy. Fixation was performed as previously described by Lara-Mondragón, et. al. [14]. Fixation began with vacuum infiltration of a solution containing 0.001% (v/v) Tween 20, 2.5% (w/v) Glutaraldehyde, 2% (w/v) Formaldehyde, and 0.025 M piperazine-N,N'-bis(2-ethanesulfonic acid) (PIPES) buffer (pH 7.2) for 2 hours followed by solution replacement and overnight incubation at 4°C. The following day, samples were washed

for 10 min in 0.025 M phosphate buffer followed by a 20 min wash in 0.025 M PIPES solution (pH 7.2) and then dehydrated via ethanol series (25%, 35%, 50%, 70%, 80%, 90%, 3x100%). Infiltration with liquid resin white (LRw, EMS #14381) occurred via incubation in solutions of resin and ethanol for 24 hours. The ratio of resin to ethanol was increased each day until fibers were fully infiltrated with resin over the course of 7 days and then oven cured for 24 hours at 58°C. After fixation and mounting, fibers were ultramicrotomed with a freshly broken glass knife to a thickness of 50 µm. A 1% toluidine blue solution was used to stain the sections for imaging. Transmission light microscopy was performed at 20x magnification on a Leica DM5500 upright microscope system. At least three cross-sections were taken per sample for analysis.

Image analysis of transmission light micrographs was performed with ImageJ Fiji software. Measurements were taken to record the area and diameters of each technical fiber (D1 = large diameter & D2 = small diameter), the area of elementary fiber, as well as the area and diameters of each lumen visible within the cross-section (d1 = large diameter, d2 = small diameter). At least 10 measurements of each fiber attribute were taken per cross-section. Specimens where the lumen was obscured or folded (due to sample preparation) were excluded. The percentage of cellular area containing lumen was recorded on at least three technical fiber cross-sections per sample.

Results and Discussion

Flax fibers were treated in the presence of supercritical CO₂ (scCO₂) at 27.6 MPa for 24 hours and their resulting properties were characterized via single fiber tensile testing. Treatment resulted in a 33% increase in fiber tensile modulus and a 40% improvement in tensile strength (Table 3).

Table 3: Single fiber tensile performance of flax fibers before and after treatment in supercritical fluid at 27.6 Mpa for 24 hours.

	Tensile Modulus		Ultimate Strength	
	(Gpa)		(Mpa)	
Untreated	23.4	± 7.1	377	± 137
scCO₂	31.1	± 9.9	529	± 266

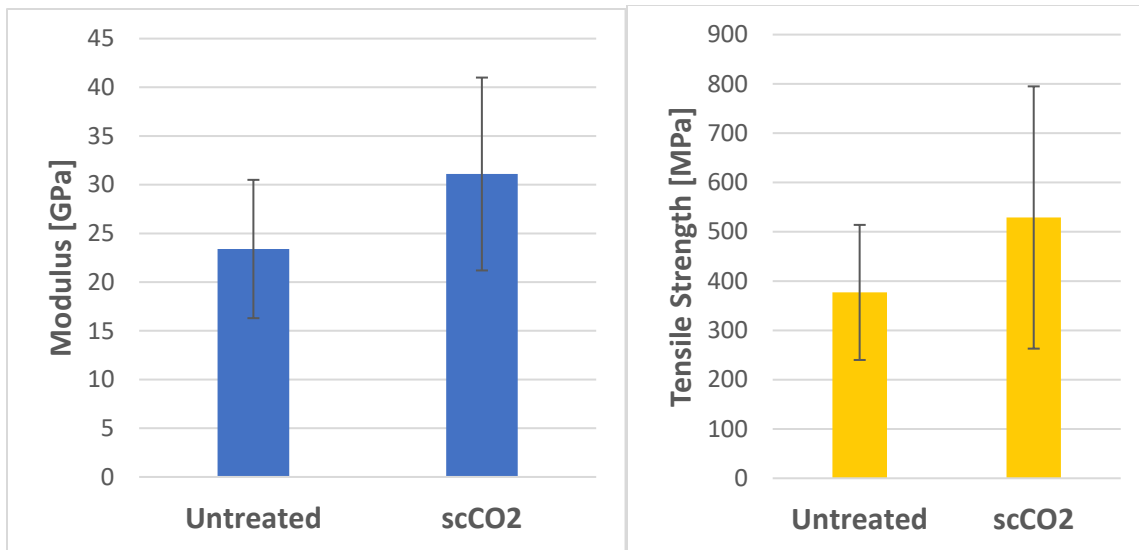


Figure 4: Improvements to modulus and tensile strength of fibers after supercritical fluid treatment

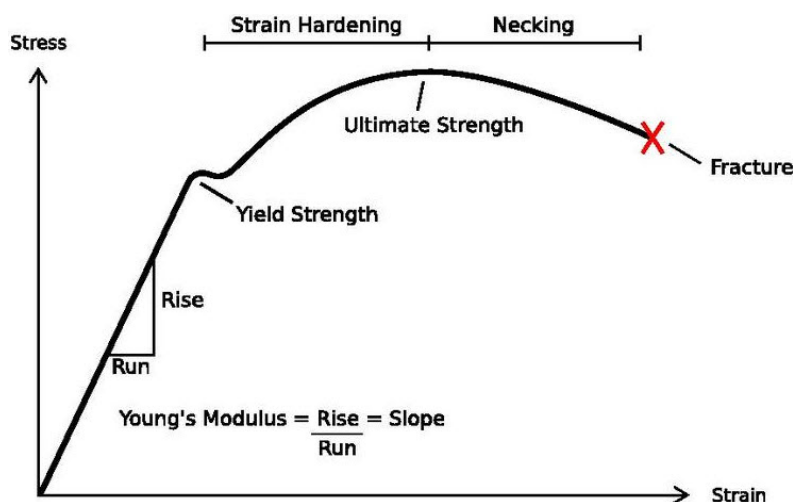


Figure 5: Schematic of stress-strain curve. The ultimate, or tensile strength represents the maximum stress value before failure. The modulus is measured as the slope of the linear (elastic) region of the curve [15].

To understand the mechanisms behind fiber property improvements, the dimensions and morphology of flax fibers were evaluated before and after treatment in scCO₂. Fibers underwent fixation, microtomy, transmission light microscopy, and image analysis as shown in Figure 6. Image analysis was performed on fiber cross-sections to quantify changes to technical fiber dimensions (D1 = large diameter, D2 = small diameter), technical fiber area, elementary fiber (cellular) area, lumen area, and lumen dimensions (d1 = large diameter, d2 = small diameter) (Table 4). Treatment resulted in similar reductions in elementary fiber cross-sectional area and technical fiber cross-sectional area. Elementary fiber area was reduced by 7.2% and technical fiber cross-sectional area was reduced by 7.9% upon treatment. However, image analysis

showed that the smaller technical fiber diameter, D2, was more significantly reduced than D1 during treatment (Figure 2). Specifically, D2 was reduced by an average of 11 μm , while D1 was reduced by an average of 0.8 μm , suggesting that differences in cellular structure along the two axes is contributing to the different responses to treatment. For example, the larger diameter of the lumen (d1) within technical fibers is commonly aligned with the larger diameter of the fiber (D1). Visualization and measurement of lumen dimensions shows that treatment in scCO_2 visibly collapses the lumen. The smaller diameter of the lumen (d2) was reduced by approximately 43% while the larger lumen diameter (d1) was reduced by $\sim 24\%$ (Table 4). The larger reduction in lumen d2 than d1 is consistent with the larger reduction in technical fiber diameter D2 vs D1. These data show that the pressure differential between the fiber's outer surface and the insulated closed lumen resulted in lumen collapse.

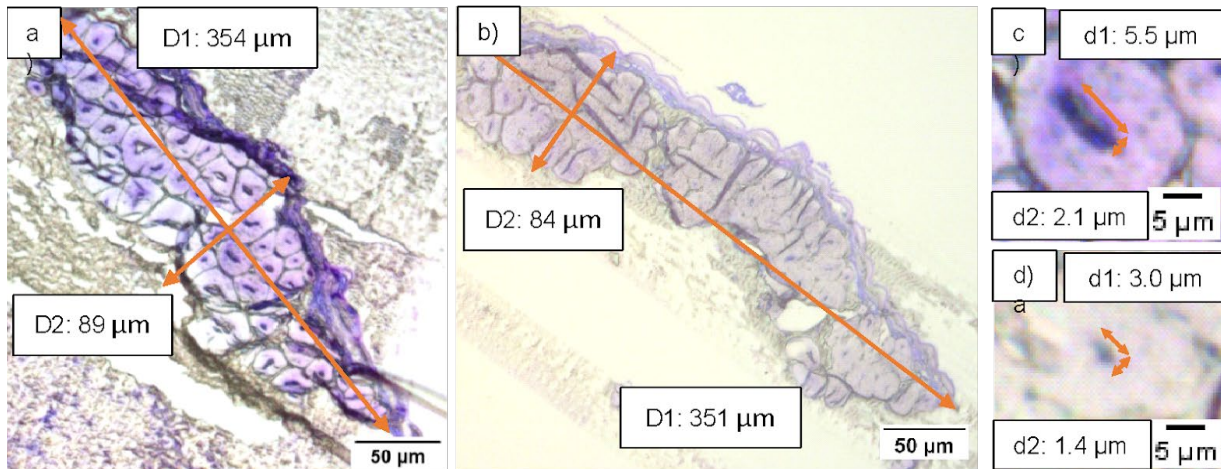


Figure 6: Flax fiber cellular morphology shown via fiber fixation and microtoming. a) Untreated fiber labeled with fiber diameters D1 and D2, b) scCO_2 treated fiber, c) untreated fiber lumen, labeled with lumen diameters d1 and d2, d) scCO_2 treated fiber lumen. Treatment with scCO_2 appears to result in collapse of lumen, reducing fiber porosity.

Table 4: Analysis of changes to cell (elementary fiber) and lumen size due to technical fiber treatment in scCO₂.

	Untreated	scCO ₂	Change due to scCO ₂ treatment
Technical Fiber Area [μm ²]	25250 ± 2085	23258 ± 1865	-7.9%
Elementary Fiber (cellular) Area [μm ²]	314.9 ± 106	292.2 ± 102	-7.2%
Lumen Area [μm ²]	10.50 ± 10.8	3.91 ± 4.2	-63%
Lumen diameter – d1 [μm]	5.90 ± 1.3	4.47 ± 1.4	-24%
Lumen diameter – d2 [μm]	2.30 ± 0.6	1.32 ± 0.5	-43%

We hypothesized that the treatment was not only causing collapse of the lumens in each technical fiber, but also contributing to consolidation of micro/meso porosity and/or free volume within the fibers. To evaluate the effects of treatment on porosity, the micro/mesoporosity and surface area of the fibers were evaluated via nitrogen physisorption. The bulk density of untreated and scCO₂ treated fibers was measured to be ~0.79 g/cm³ for both samples. Using the bulk density and pore volume measurements from gas physisorption, the contribution to total fiber porosity from micro/ mesopores was calculated using Equation 2. While macroporosity (the lumen) is reduced by ~63% upon treatment, micro/meso porosity was reduced by ~27%. Overall, flax technical fiber porosity is reduced by ~50% from treatment in scCO₂ (Table 5). It is likely that this reduction in porosity led to the observed improvements in fiber mechanical properties since pores act as stress concentrators that can cause premature failure.

$$\varphi = \frac{V_p}{V_T} = \frac{V_{po}+V_{pc}}{V_f+V_{po}V_{pc}} = \frac{\frac{V_{po}+V_{pc}}{m}}{\frac{V_f+V_{po}+V_{pc}}{m}} = \frac{V_{po}+V_{pc}}{m} * \rho_T \quad (2)$$

φ = porosity, V_p = pore volume, V_T = total (bulk) volume, V_{po} = open pore volume, V_{pc} = closed pore volume, V_f = fiber volume, m = sample mass, ρ_T = bulk density

Table 5: Summary of fiber porosity and density, before and after treatment in supercritical CO₂ (27.6 MPa, 60°C, 24hr).

	Macroporosity (%)	Micro & Mesoporosity (%)	Total Porosity (%)	Skeletal Density (g/cm ³)
Untreated	3.1	1.5	4.6	1.371 ± 0.027
scCO₂	1.2	1.1	2.3	1.442 ± 0.014

Conclusions

We developed a treatment method to improve the mechanical performance of flax fibers. Using supercritical CO₂, we achieved a 33% increase in fiber modulus and a 40% increase in tensile strength. The high-pressure fluid is believed to compact and reduce the fiber cross-sectional area, resulting in less porosity to initiate cracks and better properties. This is a step towards replacing synthetic fibers, such as glass fibers, to produce composite materials with lower carbon footprints. Importantly, this technique is simple and inexpensive, making it suitable to implement in a large-scale commercial application. In addition, the use of supercritical CO₂ as a treatment fluid provides a much-needed way for companies to get rid of captured CO₂, further reducing the greenhouse gas emissions from their operations. Hopefully, this study can help advance the field of natural fiber-reinforced composites, leading to more widespread usage in structural applications. Future work will investigate the effects of other treatment parameters, such as higher pressures, temperatures, longer fibers, other treatment fluids, and utilizing nanomaterials to further improve properties.

References

1. "What the IPCC report means for global action on 1.5°C". *Chatham House*, retrieved on 4/17/2023 from https://www.chathamhouse.org/2023/03/what-ipcc-report-means-global-action?gclid=CjwKCAjw3POhBhBQEiwAqTCuBjeBZdIG94BMDgNBkN6kELCw8z_xtNcvfMOemf6068mN13yWuFhG9hoC6gYQAvD_BwE
2. "Developing nations say they're owed for climate damage. Richer nations aren't budging". *NPR*, retrieved on 4/17/2023 from <https://www.npr.org/2021/11/11/1054809644/climate-change-cop26-loss-and-damage>
3. "Greenhouse Gas Emissions by Country 2023". *World Population Review*, retrieved on 4/17/2023 from <https://worldpopulationreview.com/country-rankings/greenhouse-gas-emissions-by-country>
4. "Fast facts on transportation greenhouse gas emissions". *EPA*, retrieved on 4/17/2023 from <https://www.epa.gov/greenvehicles/fast-facts-transportation-greenhouse-gas-emissions>
5. "Electric vehicles drive performance polymers". *Chemical Engineering*, retrieved on 4/17/2023 from <https://www.chemengonline.com/electric-vehicles-drive-performance-polymers/?printmode=1>
6. "The Inflation Reduction Act: Clean Vehicle Credits". *Center for Automotive Research*, retrieved on 4/18/2023 from https://www.cargroup.org/publication/the-inflation-reduction-act-clean-vehicle-credits/?gclid=CjwKCAjw_ihBhADEiwAXEazJtCxgqsukVPs4e7pLx_b_rLttiUFJOkhbwV1iGWCzT-QUGpi0Y3RGxoCeJ4QAvD_BwE

7. "Shape Corp produces industry-first carbon fiber bumper for 2020 Chevrolet Corvette Stingray". *Shape Corp*, retrieved on 4/18/2023 from <https://www.shapecorp.com/shape-corp-produces-industry-first-carbon-fiber-bumper-for-2020-chevrolet-corvette-stingray/>
8. Langhorst, A., Harrison, E., Singhal, A., Banu, M. & Taub, A. "Reinforcement of Natural Fibers via Supercritical Fluid Infiltration of Nanoparticles". *American Society for Composites Thirty-Seventh Technical Conference* (2022).
9. Wambua, P., Ivens, J. & Verpoest, I. "Natural fibres: Can they replace glass in fibre reinforced plastics?" *Compos. Sci. Technol.* **63**, 1259–1264 (2003).
10. Richely, E. *et al.* "Novel insight into the intricate shape of flax fibre lumen". *Fibers* **9**, (2021).
11. François, C. *et al.* "Can supercritical carbon dioxide be suitable for the green pretreatment of plant fibres dedicated to composite applications?" *J. Mater. Sci.* **55**, 4671–4684 (2020).
12. American Society for Testing and Materials. "Standard Test Method for Tensile Strength and Young's Modulus of Fibers". *Astm C1557-14* 1–10 (2014).
13. Singhal, A., Banu, M. & Taub, A. "Improving the process of stem breaking for damage reduction in extracted natural fibers". *J. Manuf. Process.* **86**, 143–151 (2023).
14. Lara-Mondragón, C. M. & MacAlister, C. A. "Arabinogalactan glycoprotein dynamics during the progamic phase in the tomato pistil". *Plant Reprod.* **34**, 131–148 (2021).
15. "Describe/draw the stress-strain curve of aluminum vs. steel on the same graph". *Hardware interviews*, retrieved on 4/19/2023 from <https://www.hardwareinterviews.fyi/t/describe-draw-the-stress-strain-curve-of-aluminum-vs-steel-on-the-same-graph/113>